Contribution from the Laboratoire de Chimie de Coordination du CNRS, UP 8241 liée par conventions à l'Université Paul Sabatier et à l'Institut National Polytechnique, 205 route de Narbonne, 31077 Toulouse Cedex, France

Structural Characterization and Magnetic Study (EPR and Static Susceptibility Measurements) of a Novel Ferric Spin-Crossover Complex: Bis(7-amino-4-methyl-5-aza-3-hepten-2-onato(1-))iron(III) Tetraphenylborate

Jean-Pierre Costes,* Françoise Dahan, and Jean-Pierre Laurent

Received July 11, 1989

EPR and magnetic susceptibility studies show that $[Fe(AE)_2]BPh_4$, where AE is the monoanionic Schiff base derived from 2,4-pentanedione and 1,2-diaminoethane, is a ferric spin-crossover complex. Indeed, we observe a gradual but nearly complete transition from the high-spin ($S = {}^5/_2$) to the low-spin state ($S = {}^1/_2$) with decreasing temperature. The number and positions of the EPR lines in the solid state are consistent with the presence of two high-spin and one low-spin species. The compound $[C_{14}H_{26}FeN_4O_2]C_{24}H_{20}B$ crystallizes in the triclinic space group $P\bar{1}$ with $a = 12.768$ (1) Å, $b = 13.559$ (1) Å, $c = 11.092$ (1) Å, $\alpha = 107.87$ (1)°, $\beta = 107.67$ (1)°, $\gamma = 79.01$ (1)°, and $Z = 2$. The two tridentate ligands (with a meridional configuration) lie in approximately orthogonal planes around the ferric ion, providing the metal center with a pseudooctahedral geometry. The metal-ligand bond lengths are in good agreement with the presence of high-spin species at room temperature.

Introduction

Six-coordinate d^5 iron(III) Schiff base complexes of general types $[Fe(N_2O_2)L_2]^{+1-5}$ [where (N_2O_2) is a N_2O_2 Schiff base ligand deriving from *N,N'*-ethylenebis(salicylaldimine) (Salen) or *N,N'*-ethylenebis(acetylacetone imine) (acen) and L is a monodentate ligand], $[Fe(N_2O)_2]^{+6-13}$ [(N_2O): tridentade Schiff base ligand], $[Fe(N_3O_2)L]^{+14}$ [(N_3O_2): pentadentate ligand], and $[Fe(N_4O_2)]^{+15-17}$ [(N_4O_2): hexadentate ligand] are known to display a variety of magnetic behaviors. Minor variations in all components of the complexes can lead to high-spin ($S = {}^5/_2$) or low-spin ($S = {}^1/_2$) states on Fe(III) and also to spin-crossover behavior.[18] The O_2N_4 donor set likely produces an overall ligand field close to the crossover point, as it has been found for related $[N_6]$ porphyrin adducts.[20-22]

In addition to the influence in the spin-crossover transition exerted by intramolecular and structural factors, it has been shown[8,10,11,23-25] that intermolecular effects and lattice features can also be significant in the solid state to influence the characteristics of the spin-crossover transformation. Particular attention has been recently paid to the spin-state interconversion rates (see refs 6,9,26 and references therein).

This paper is devoted to a novel example of a complex with an $Fe^{III}N_4O_2$ chromophore, i.e. bis(7-amino-4-methyl-5-aza-3-hepten-2-onato(1-))iron(III) tetraphenylborate, abbreviated as $[(AE)_2Fe]BPh_4$ hereafter. Initially, the attention paid to this complex arose from preliminary magnetic data. Indeed, samples prepared by grinding crystals displayed abnormal magnetic moments; values ranging from ca. 3.6 μ_B at 5 K to 5.0 μ_B at 290 K had been observed. This prompted us to make a more accurate study including a structural determination and the measurement of the magnetic properties on a "nonperturbed" sample directly obtained as a powder.

Table I. Crystallographic Data for $[C_{14}H_{26}FeN_4O_2]C_{24}H_{20}B$

chem formula: $BC_{38}FeH_{46}N_4O_2$	space group $P\bar{1}$ (No. 2)
fw 657.47	$T = 20$ °C
$a = 12.768$ (1) Å	$\lambda = 0.71073$ Å
$b = 13.559$ (1) Å	$\rho_{meas} = 1.28$ g/cm^3
$c = 11.092$ (1) Å	$\rho_{calc} = 1.261$ g/cm^3
$\alpha = 107.87$ (1)°	$\mu = 4.7$ cm^{-1}
$\beta = 107.67$ (2)°	transm coeff = 0.97-1.00
$\gamma = 79.01$ (1)°	$R(F_o) = 0.035$
$V = 1731.3$ (7) Å^3	$R_w(F_o) = 0.036$
$Z = 2$	

Experimental Section

Compound Preparation. Bis(7-amino-4-methyl-5-aza-3-hepten-2-onato(1-))iron(III) Tetraphenylborate ($[Fe(AE)_2]BPh_4$). To a methanolic solution (70 mL) of AEH[27] (1.41×10^{-2} M, 2 g) and triethylamine (2 mL) was added anhydrous iron(III) chloride (7×10^{-3} M, 1.14 g) dissolved in methanol (30 mL). The solution was stirred and heated for 20 min, after which sodium tetraphenylborate (7×10^{-3} M, 2.4 g) in methanol was added at once. The resulting solution was evaporated, yielding a sticky product. Then 80 mL of tetrahydrofuran was added. Addition of water to the filtered solution induced the precipitation of a purple powder, which was filtered off and dried under reduced pressure. Yield: 80%. Anal. Calcd for $C_{38}H_{46}BFeN_4O_2$: C, 69.4; H, 7.0; Fe, 8.5; N, 8.5. Found: C, 68.1; H, 7.0; Fe, 8.4; N, 8.6. Part of the powder was dissolved in dichloromethane. An equivalent amount of diethyl ether was added and the solution was left overnight, yielding crystals suitable for X-ray analysis.

Physical Measurements. Microanalyses were performed by the Service Central de Microanalyse du CNRS, Lyon, France. Magnetic susceptibility data were collected on powdered samples of the compound

(1) Nishida, Y.; Oshio, S.; Kida, S. *Bull. Chem. Soc. Jpn.* **1977**, *50*, 119.
(2) Ohshio, H.; Maeda, Y.; Takashima, Y. *Inorg. Chem.* **1983**, *22*, 2684.
(3) Kennedy, B. J.; McGrath, A. C.; Murray, K. S.; Skelton, B. W.; White, A. H. *Inorg. Chem.* **1987**, *26*, 483.
(4) Maeda, Y.; Takashima, Y.; Matsumoto, N.; Ohyoshi, A. *J. Chem. Soc., Dalton Trans.* **1986**, 1115.
(5) Kennedy, B. J.; Brain, G.; Horn, E.; Murray, K. S.; Snow, M. R. *Inorg. Chem.* **1985**, *24*, 1647.
(6) Maeda, Y.; Tsutsumi, N.; Takashima, Y. *Inorg. Chem.* **1984**, *23*, 2440.
(7) Federer, W. D.; Hendrickson, D. N. *Inorg. Chem.* **1984**, *23*, 3861.
(8) Federer, W. D.; Hendrickson, D. N. *Inorg. Chem.* **1984**, *23*, 3870.
(9) Timken, M. D.; Strouse, C. E.; Soltis, S. M.; Daverio, S. A.; Hendrickson, D. N.; Abdel-Mawgoud, A. M.; Wilson, S. R. *J. Am. Chem. Soc.* **1986**, *108*, 395.
(10) Haddad, M. S.; Lynch, M. N.; Federer, W. D.; Hendrickson, D. N. *Inorg. Chem.* **1981**, *20*, 123.
(11) Haddad, M. S.; Federer, W. D.; Lynch, M. N.; Hendrickson, D. N. *Inorg. Chem.* **1981**, *20*, 131.
(12) Timken, M. D.; Abdel-Mawgoud, A. M.; Hendrickson, D. N. *Inorg. Chem.* **1986**, *25*, 160.
(13) Timken, M. D.; Hendrickson, D. N.; Sinn, E. *Inorg. Chem.* **1985**, *24*, 3947.
(14) Matsumoto, N.; Ohta, S.; Yoshimura, C.; Ohyoshi, A.; Kohata, S.; Okawa, H.; Maeda, Y. *J. Chem. Soc., Dalton Trans.* **1985**, 2575.
(15) Dose, E. V.; Murphy, K. M. M.; Wilson, L. J. *Inorg. Chem.* **1976**, *15*, 2622.
(16) Sinn, E.; Sim, G.; Dose, E. V.; Tweedle, M. F.; Wilson, L. J. *J. Am. Chem. Soc.* **1978**, *100*, 3375.
(17) Binstead, R. A.; Beattie, J. K.; Dewey, T. G.; Turner, D. H. *J. Am. Chem. Soc.* **1980**, *102*, 6442.
(18) Other spin states can be found: intermediate spin, quantum mixed $S = {}^3/_2, {}^5/_2$ intermediate spin.
(19) Gregson, A. K. *Inorg. Chem.* **1981**, *20*, 81 and references therein.
(20) Scheidt, W. R.; Geiger, D. K.; Haller, K. J. *J. Am. Chem. Soc.* **1982**, *104*, 495.
(21) Scheidt, W. R.; Geiger, D. K.; Hayes, R. G.; Lang, G. *J. Am. Chem. Soc.* **1983**, *105*, 2625.
(22) Geiger, D. K.; Lee, Y. J.; Scheidt, W. R. *J. Am. Chem. Soc.* **1984**, *106*, 6339.
(23) Gütlich, P. *Struct. Bonding (Berlin)* **1981**, *44*, 83.
(24) König, E.; Ritter, G.; Kulshreshtha, S. K.; Nelson, S. M. *J. Am. Chem. Soc.* **1983**, *105*, 1924.
(25) Sorai, M.; Seki, S. *J. Phys. Chem. Solids* **1974**, *35*, 555.
(26) Timken, M. D.; Abdel-Mawgoud, A. M.; Hendrickson, D. N. *Inorg. Chem.* **1986**, *25*, 160.
(27) Cros, G.; Costes, J. P. *C. R. Seances Acad. Sci., Ser. 2* **1982**, *294*, 173.

0020-1669/90/1329-2448$02.50/0

Table II. Fractional Atomic Coordinates with Estimated Standard Deviations in Parentheses

atom	x/a	y/b	z/c
Fe	0.77728 (3)	0.33004 (3)	0.32563 (4)
O(1)	0.7632 (2)	0.4417 (2)	0.4795 (2)
C(1)	0.8376 (3)	0.4806 (2)	0.5839 (3)
C(2)	0.9465 (3)	0.4479 (2)	0.6085 (3)
C(3)	0.9985 (3)	0.3619 (2)	0.5279 (3)
C(4)	0.7921 (3)	0.5703 (3)	0.6806 (4)
C(5)	1.1229 (3)	0.3426 (3)	0.5752 (4)
N(1)	0.9441 (2)	0.3016 (2)	0.4206 (2)
C(6)	1.0042 (3)	0.2153 (3)	0.3413 (3)
C(7)	0.9279 (3)	0.1348 (3)	0.2597 (3)
N(2)	0.8251 (2)	0.1854 (2)	0.1900 (3)
O(2)	0.8087 (2)	0.4086 (2)	0.2236 (2)
C(8)	0.7556 (3)	0.4149 (2)	0.1057 (3)
C(9)	0.6514 (3)	0.3894 (3)	0.0443 (3)
C(10)	0.5809 (3)	0.3560 (2)	0.0970 (3)
C(11)	0.8194 (3)	0.4560 (3)	0.0403 (4)
C(12)	0.4649 (3)	0.3415 (3)	0.0107 (4)
N(3)	0.6139 (2)	0.3390 (2)	0.2128 (3)
C(13)	0.5376 (3)	0.3092 (3)	0.2695 (4)
C(14)	0.5868 (3)	0.2255 (3)	0.3318 (4)
N(4)	0.7038 (2)	0.2375 (2)	0.4021 (3)
B	0.2684 (3)	0.8826 (2)	0.3017 (3)
C(15)	0.2583 (1)	0.9536 (2)	0.4528 (2)
C(16)	0.1547 (1)	0.9934 (2)	0.4749 (2)
C(17)	0.1465 (1)	1.0531 (2)	0.5996 (2)
C(18)	0.2419 (1)	1.0728 (2)	0.7021 (2)
C(19)	0.3456 (1)	1.0330 (2)	0.6799 (2)
C(20)	0.3537 (1)	0.9734 (2)	0.5553 (2)
C(21)	0.3690 (1)	0.7819 (1)	0.3154 (2)
C(22)	0.3477 (1)	0.6806 (1)	0.2976 (2)
C(23)	0.4352 (1)	0.6029 (1)	0.3164 (2)
C(24)	0.5440 (1)	0.6265 (1)	0.3529 (2)
C(25)	0.5653 (1)	0.7279 (1)	0.3707 (2)
C(26)	0.4778 (1)	0.8056 (1)	0.3519 (2)
C(27)	0.3053 (2)	0.9579 (1)	0.2295 (2)
C(28)	0.3450 (2)	0.9100 (1)	0.1189 (2)
C(29)	0.3698 (2)	0.9705 (1)	0.0518 (2)
C(30)	0.3549 (2)	1.0790 (1)	0.0953 (2)
C(31)	0.3152 (2)	1.1269 (1)	0.2058 (2)
C(32)	0.2904 (2)	1.0664 (1)	0.2729 (2)
C(33)	0.1432 (2)	0.8426 (1)	0.2112 (2)
C(34)	0.0871 (2)	0.8760 (1)	0.0991 (2)
C(35)	−0.0157 (2)	0.8427 (1)	0.0250 (2)
C(36)	−0.0625 (2)	0.7760 (1)	0.0631 (2)
C(37)	−0.0065 (2)	0.7426 (1)	0.1752 (2)
C(38)	0.0964 (2)	0.7759 (1)	0.2493 (2)

with use of a Faraday-type magnetometer using mercury tetrakis(thiocyanato)cobaltate (susceptibility at 20 °C: 16.44×10^{-6} cm^3 mol^{-1}) as susceptibility standard. Data were corrected for diamagnetism of the ligands and anions, estimated from Pascal constants[28] to be -317×10^{-6} cm^3 mol^{-1}. EPR spectra were recorded at X-band frequency (9.4–9.5 GHz) with a Bruker 200 TT spectrometer.

Magnetic susceptibility measurements of the compound in solution were determined by nuclear magnetic resonance spectroscopy using dichloromethane as solvent and tetramethylsilane as indicator.

X-ray Structure Analysis. The experimental parameters are listed in Table I. A dark blue crystal (length 0.35 mm; hexagonal basis 0.20 × 0.10 × 0.10 mm) was sealed on a glass fiber and transferred to a CAD4 Enraf-Nonius diffractometer automated with a MicroVax 2000 computer.

The unit cell was refined by using 25 reflections in the 2θ range 19–26°. A total of 5116 intensity data were collected in the $\theta/2\theta$ scan mode (scan width 0.75° + 0.35° tan θ; scan speed 1.1–8.4° min^{-1}) up to $2\theta = 47°$. A set of three standard reflections was measured every 2 h of exposure time, with no noticeable change in intensity observed during the collection. Lorentz–polarization and empirical absorption[29] corrections were made with SDP.[30]

The structure was solved by a Patterson map calculation, and the refinement and difference-Fourier processes were performed with SHELX76.[31] Of the 5116 reflections collected, 3866 reflections having $I > 3\sigma(I)$ were used. The atomic scattering factors are those of ref 32 for heavy atoms, including anomalous dispersion effects, and those of ref 33 for hydrogens. Full-matrix least-squares techniques were used with phenyl rings refined as isotropic rigid groups (C–C = 1.395 Å). All H atoms were observed, but they were introduced into calculations in constrained geometry (C–H = 0.97 Å) with a temperature factor of U = 0.065 Å^2, kept fixed. All other atoms were refined anisotropically. The refinement converged with a mean shift/esd of 0.05 on the final cycle with 247 variable parameters. With unit weights, the fit led to an S value of 0.92, and no other weighting scheme was used. The maximum residual peak was 0.5 e/Å^3. Fractional atomic coordinates are given in Table II. All calculations were performed on a Vax 730 computer.

Table III. Selected Bond Lengths (Å) and Angles (deg) with Estimated Standard Deviations in Parentheses

Fe–O(1)	1.932 (2)	Fe–O(2)	1.937 (3)
Fe–N(1)	2.090 (2)	Fe–N(2)	2.184 (2)
Fe–N(3)	2.085 (2)	Fe–N(4)	2.182 (4)
O(1)–Fe–O(2)	99.5 (1)	O(2)–Fe–N(4)	165.79 (8)
O(1)–Fe–N(1)	88.20 (8)	N(1)–Fe–N(2)	79.09 (9)
O(1)–Fe–N(2)	164.9 (1)	N(1)–Fe–N(3)	172.25 (9)
O(1)–Fe–N(3)	99.34 (9)	N(1)–Fe–N(4)	100.1 (1)
O(1)–Fe–N(4)	86.1 (1)	N(2)–Fe–N(3)	93.19 (9)
O(2)–Fe–N(1)	93.1 (1)	N(2)–Fe–N(4)	88.0 (1)
O(2)–Fe–N(2)	89.5 (1)	N(3)–Fe–N(4)	78.7 (1)
O(2)–Fe–N(3)	87.4 (1)		
O(1)–C(1)	1.292 (3)	O(2)–C(8)	1.299 (4)
C(1)–C(2)	1.347 (5)	C(8)–C(9)	1.354 (5)
C(1)–C(4)	1.509 (5)	C(8)–C(11)	1.510 (7)
C(2)–C(3)	1.423 (4)	C(9)–C(10)	1.413 (6)
C(3)–C(5)	1.513 (4)	C(10)–C(12)	1.511 (4)
C(3)–N(1)	1.299 (3)	C(10)–N(3)	1.302 (5)
N(1)–C(6)	1.472 (4)	N(3)–C(13)	1.479 (6)
C(6)–C(7)	1.491 (5)	C(13)–C(14)	1.451 (6)
C(7)–N(2)	1.469 (4)	C(14)–N(4)	1.474 (4)
Fe–O(1)–C(1)	130.4 (2)	Fe–O(2)–C(8)	128.1 (2)
O(1)–C(1)–C(2)	125.4 (3)	O(2)–C(8)–C(9)	124.5 (4)
O(1)–C(1)–C(4)	113.7 (3)	O(2)–C(8)–C(11)	114.2 (3)
C(2)–C(1)–C(4)	120.9 (3)	C(9)–C(8)–C(11)	121.3 (3)
C(1)–C(2)–C(3)	126.1 (3)	C(8)–C(9)–C(10)	126.9 (3)
C(2)–C(3)–N(1)	123.1 (3)	C(9)–C(10)–N(3)	122.0 (3)
C(2)–C(3)–C(5)	116.1 (2)	C(9)–C(10)–C(12)	115.8 (3)
N(1)–C(3)–C(5)	120.8 (3)	N(3)–C(10)–C(12)	122.4 (4)
C(3)–N(1)–C(6)	119.8 (2)	C(10)–N(3)–C(13)	121.4 (3)
C(3)–N(1)–Fe	125.7 (2)	C(10)–N(3)–Fe	125.5 (3)
Fe–N(1)–C(6)	113.4 (2)	Fe–N(3)–C(13)	112.6 (2)
N(1)–C(6)–C(7)	109.0 (3)	N(3)–C(13)–C(14)	112.8 (3)
C(6)–C(7)–N(2)	109.1 (3)	C(13)–C(14)–N(4)	111.0 (3)
C(7)–N(2)–Fe	108.5 (2)	C(14)–N(4)–Fe	112.6 (2)

Results and Discussion

Molecular and Crystal Structure. The lattice of this complex consists of well-defined $[(AE)_2Fe]^+$ cations and $[BPh_4]^-$ anions. The structure and numbering system for the cation are shown in Figure 1, and selected bond lengths and angles are given in Table III.

It is evident from Table III that the two tridentate ligands (AE), which lie in approximately orthogonal planes about the ferric ion, provide the metal center with a pseudooctahedral geometry. The oxygen atoms on the two ligands are located cis to each other whereas the imino nitrogen atoms are trans. This geometry has been observed in all the complexes[13,34,35] where two N_2O tridentate Schiff base ligands with ethylene linkages between imine and amine nitrogen donors are present and also for ferric complexes with hexadentate N_4O_2 ligands derived from triethylenetetr-

(28) Pascal, P. *Ann. Chim. Phys.* **1910**, *19*, 5.
(29) North, A. C. T.; Phillips, D. C.; Mathews, F. S. *Acta Crystallogr.* **1968**, *A24*, 351.
(30) Frentz, B. A. *SDP. Structure Determination Package*; Enraf-Nonius: Delft, Holland, 1982.
(31) Sheldrick, G. M. *SHELX76. Program for Crystal Structure Determination*; University of Cambridge; Cambridge, England, 1976.
(32) *International Tables for X-ray Crystallography*; Ibers, J. A., Hamilton, W. C., Eds.; Kynoch Press: Birmingham, England, 1974; Vol. IV.
(33) Stewart, R. F.; Davidson, E. R.; Simpson, W. T. *J. Chem. Phys.* **1965**, *42*, 3175.
(34) Sim, P. G.; Sinn, E.; Petty, R. H.; Merril, C. L.; Wilson, L. J. *Inorg. Chem.* **1981**, *20*, 1213.
(35) Summerton, A. P.; Diamantis, A. A.; Snow, M. R. *Inorg. Chim. Acta* **1978**, *27*, 123.

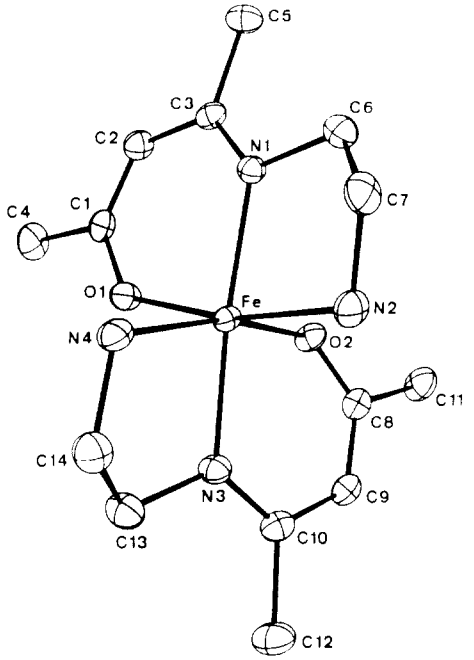

Figure 1. ORTEP plot of the $[Fe(AE)_2]^+$ cation with the atomic numbering scheme. H atoms were omitted for clarity.

amine.[16] A completely trans ligand atom configuration has been recently reported for a complex involving a 1,3-propanediyl bridge.[9]

The deviation from octahedral symmetry of the FeN_4O_2 unit is indicated by bond lengths and angles. The angles O(1)–Fe–N(2), O(2)–Fe–N(4), and N(1)–Fe–N(3) all deviate markedly from the ideal value of 180°, the smallest deviation being observed for N(1)–Fe–N(3). The 12 angles at the iron atom involving adjacent donor atoms range from 99.5 (1) to 78.7 (1)° compared to the 90° value required for a perfect octahedron.

The three planes defined by the three groups of four donors deviate from true planarity. They assume a tetrahedral deformation that becomes increasingly greater in going from plane I [N(1)O(2)N(3)N(4)] to plane II [O(1)N(1)N(2)N(3)] and plane III [O(1)N(2)O(2)N(4)]. In this last case, the distances of the donor atoms to the mean plane range from ca. 0.19 to ca. 0.31 Å whereas the iron atom lies almost perfectly in the plane. In the two former cases, the metal center is displaced from the related mean planes by 0.1071 (4) and 0.0878 (4) Å, respectively. The three planes are not far from being orthogonal to each other with dihedral angles of 92.8 (I, II), 90.8 (I, III), and 87.4° (II, III).

The metal–ligand bond lengths are uneven: the two Fe–O bonds are by far the shortest (1.93 Å average) and the bonds to the amino nitrogen atoms (2.17 Å average) are longer than those to the imino nitrogen (2.10 Å average). This trend is very similar to those observed in the related ferric N_4O_2 system.[9,13,34,36] Furthermore, these bond lengths are in good agreement with the magnetic susceptibility data to show that, at room temperature, the complex is essentially high-spin.

Indeed, the average Fe–ligand bond lengths of 2.07 Å characterizing the present complex are almost identical with the value generally attributed to the high-spin state in ferric N_4O_2 systems, i.e. 2.08 Å, while a value of 1.95 Å would be expected for a low-spin species.

Bond lengths and angles within the AE moieties are similar to those previously obtained for various copper complexes.[37] The acetylacetone rings are planar with no atom deviating from the related least-squares plane by more than 0.04 Å. The five-membered rings defined by the iron atom and the ethylenediamine bridge are definitely nonplanar but display a gauche conformation.

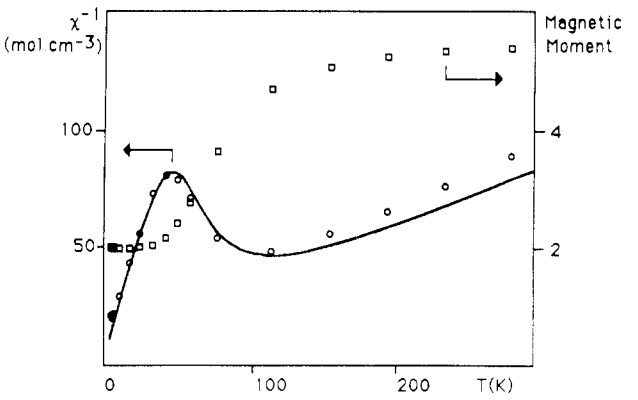

Figure 2. Magnetic moment (□) and reciprocal susceptibility (○) as a function of temperature for $[Fe(AE)_2]BPh_4$. The solid lines are the calculated values best fit to the model of Martin et al. using the parameter values given in the text.

Magnetic Susceptibility. The variable-temperature magnetochemical data have been obtained in the range 5–280 K for the powdered sample. The overall shape of the μ vs T curve and the "minimum" dependence of χ^{-1} vs T that are displayed in Figure 2 are as expected for a gradual but nearly complete transition from a high-spin ($S = {}^5/_2$) to a low-spin ($S = {}^1/_2$) state with decreasing temperature.

These data have been analyzed by means of the simple noninteracting model developed by Martin.[38] We see from Figure 2 that, in the temperature range 5–150 K, which encompasses the most significant part of the transformation, a reasonable fit could be obtained with values of the $({}^6A_{1g}-{}^2T_{2g})$ energy separation of -55 cm^{-1}, ξ (spin–orbit coupling constant) = 280 cm^{-1}, g = 2.11, and C = 5.7 (C being the ratio of the molecular vibrational partition function for the two spin states). It may be recalled that a number of assumptions are implicit in this model, not the least of which are the assumptions of perfect octahedral symmetry and noninteraction (via spin–orbit coupling) of the energy levels. In the present case, the combined effects of molecular distortion from pure octahedral geometry and spin–orbit coupling interaction are expected to split the $^2T_{2g}$ state into three Kramers doublets. The high-spin state $^6A_{1g}$ also splits into three doublets but with much smaller splittings.

Finally, it may be considered that the levels involved in the spin transition are the lower doublet of $^2T_{2g}$ origin and the array of three doublets of $^6A_{1g}$ origin. Interestingly, the thermal variation of χ^{-1} between ca. 285 and ca. 50 K could be described by a very simple model, i.e. a Boltzmann distribution over a low-spin doublet with an associated moment of 1.9 μ_B and a high-spin multiplet with an associated moment of 5.9 μ_B. A reasonable fit to the experimental data was obtained by taking an energy separation of 170 cm^{-1} and a C value of 5.2. A more sophisticated treatment using, for instance, the interacting "mixed-spin" model developed by Harris and Gregson[19,39] might be desirable to achieve an accurate characterization of the spin states, but the essential conclusion is clear: the energies of the two states involved in the spin transition are close.

Due to the use of Evans' method,[40] the magnetic data related to solution were restricted to the range 190–290 K. First of all, it may be underlined that identical data were obtained for solutions (CH_2Cl_2) prepared from powdered samples and from crystals. In spite of this narrow range of temperatures, a significant variation of μ is observed, from 5.19 μ_B at 298 K to 3.21 μ_B at 190 K, supporting the view of a transition from a high-spin to a low-spin state.

As usual, the high-spin population (x) at a given temperature may be evaluated by assuming a simple additive property in

(36) Ito, T.; Sugimoto, M.; Ito, H.; Toriumi, K.; Nakayama, H.; Mori, W.; Sekizaki, M. *Chem. Lett.* **1983**, 121.
(37) Costes, J. P.; Serra, J. F.; Dahan, F.; Laurent, J. P. *Inorg. Chem.* **1986**, *25*, 2790.
(38) Ewald, A. H.; Martin, R. L.; Sinn, E.; White, A. H. *Inorg. Chem.* **1969**, *8*, 1837.
(39) Harris, G. *Theor. Chim. Acta* **1968**, *10*, 119.
(40) Evans, D. F. *Proc. Chem. Soc., London* **1958**, 115.

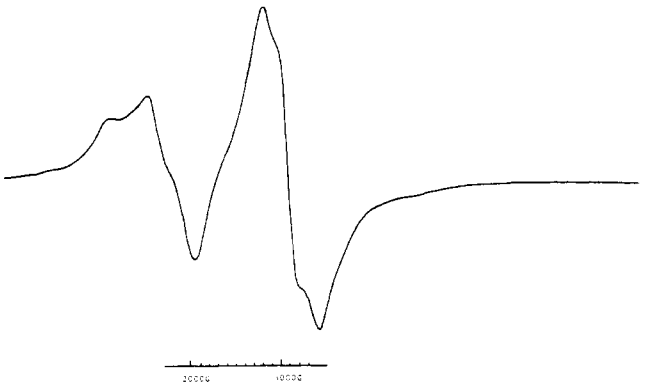

Figure 3. EPR spectrum of $[Fe(AE)_2]BPh_4$, solid state, at 90 K.

magnetic susceptibilities. Then the equilibrium constant and thermodynamic parameters can be calculated from the expressions $K = x/(1 - x)$ and $\ln K = -\Delta H/RT + \Delta S/R$, respectively. From the experimental data a straight-line plot of $\ln K$ vs T^{-1} is obtained, yielding $\Delta H = -2.57$ kcal and $\Delta S = 10.8$ cal. These values are similar to those found for related complexes involving Schiff base ligands derived from *N,N'*-ethylenebis(salicylaldimine)[9,17,41] or *N,N'*-ethylenebis(acetylacetoneimine).[2,6,15] The major contribution to the ΔH value probably reflects the changing Fe–donor atom bond distances and energy that are known to accompany spin conversion processes.

Electron Paramagnetic Resonance. At room temperature the spectrum of the powdered sample comprises a broad symmetric signal at $g \sim 4$ with a very weak feature at $g \sim 2$. Lowering the temperature results in increasing the intensity of the latter signal with respect to that of the former one. At 90 K (cf. Figure 3) both sets become resolved with effective g values of 5.80, 4.38, 3.30, 2.40, 2.20, and 1.98. In addition, broad and weak signals are discernible at $g \sim 9.8$ and 1.5. At 5 K the resolution is still improved, allowing the observation of a prominent 3*g* pattern (g = 2.42, 2.18, and 1.97) and much less intense lines at $g = 4.38$, 4.08, and 1.46. This temperature dependence of the spectral profile roughly parallels the data from susceptibility measurements and supports the view of a $^1/_2 \Leftrightarrow {}^5/_2$ spin-crossover transformation. Indeed, the 3*g* pattern at $g \sim 2$ is obviously attributable to a rhombic low-spin system whereas high-spin species are known to display characteristic signals at $g \sim 4$ or $g \sim 6$, depending on the values of their zero-field-splitting parameters (D and E).

At 4 K the high-spin signals have a very low intensity but they are reasonably well-resolved. They can be understood in terms of Wickman's analysis.[42] With the use of the eigenfunctions and expressions provided in ref 42, the three effective **g** tensors related to three Kramers doublets from the $^6A_{1g}$ state may be calculated. With $E/D = 0.25$, the following values are obtained: g_1 = 0.49, 0.38, 9.84; g_2 = 4.08, 3.76, 4.76; g_3 = 1.45, 9.38, 0.92.

A careful examination of the 5 K spectrum shows that the most intense signal of the high-spin spectrum is the one with an effective g value of 1.46, which therefore must be attributed to the lower doublet, whereas the feature with maxima at $g = 4.38$ and 4.08 results from the overlap of the three lines from the middle doublet. It is not unexpected that the other resonances at low and high fields are not clearly detected. This analysis implies that at least two doublets are populated at 5 K so that their spacing, which approaches $3D$ as E/D approaches 0.30, would be of the same order of magnitude as the thermal energy. This leads to a D value of ca. 1 cm^{-1}.

Returning to the 90 K high-spin spectrum, we note that the number of detected signals is higher than that in the 5 K spectrum. New lines are clearly seen at $g = 5.81$ and 3.28, and a broad feature appears at $g \sim 9$. They cannot be attributed to the former high-spin species characterized by $E/D = 0.25$ but may arise from a second species of lower rhombicity. Within the framework of Wickman's analysis an E/D value of 0.12 would lead to the following: g_1 = 0.11, 0.09, 9.98; g_2 = 2.09, 3.16, 5.80; g_3 = 3.42, 8.69, 1.68.

Well-resolved solution (CH_2Cl_2) spectra have only been obtained at low temperature, i.e. 100 K. In keeping with the susceptibility data, the largely predominant feature centered at $g \sim 2$ is attributed to a low-spin species. However, it is noteworthy that, in contrast to the rhombically distorted spectrum characterizing the low-spin species in powdered samples, an axial spectrum ($g_\parallel = 1.94$, $g_\perp = 2.21$) is seen in solution. In addition, the spectrum comprises a low-field signal of very low intensity with effective g values of 4.38 and 4.08. It is identical with that observed for the high-spin component of the powdered samples at 4 K. As previously reported, these data are consistent with a high degree of rhombicity ($E/D = 0.25$). At variance with the solid-state spectra, signals attributable to a second high-spin species are not detected.

A further look at the low-spin spectra is appropriate, for they provide information concerning the orbital constitution and the energetics of the Kramers doublets of $^2T_{2g}$ origin. The analysis used in the present study is that developed by Bohan.[43] It has been described in several papers and will not be reproduced here. Suffice it to say that an orbital reduction factor (k) is introduced in the Zeeman Hamiltonian and that the Hamiltonian for spin–orbit coupling and the ligand field distortions interactions is

$$\mathcal{H} = -\xi ls + (\mu/9)[3l_z^2 - l(l+1)] + (R/12)[l_+^2 + l_-^2]$$

where ξ is the spin–orbit coupling constant and μ and R are the ligand field parameters that gauge the axial and rhombic distortions, respectively.

The ordering and numbering of the g values are chosen so as to obtain physically reasonable solutions for each type of spectra and consistency between the two sets of data obtained for solid samples and solution, respectively.

For solid-state spectra, assuming that the three g values are positive and attributed according to $g_x = 2.413$, $g_y = 2.182$, and $g_z = 1.957$ leads to the conclusion that the ground Kramers doublet

$$\Psi = A|+1^+\rangle + B|\xi^-\rangle + C|-1^+\rangle$$

$$\Psi' = A|-1^-\rangle - B|\xi^+\rangle + C|+1^-\rangle$$

may be described by the following values of the orbital coefficient:

$$A = -0.097, \quad B = -0.998, \quad C = 0.033$$

The axial (μ) and rhombic (R) distortion parameters are then found to be $\mu/\xi = -8.8$ and $R/\xi = 6.4$, while the relative energies of the three states of $^2T_{2g}$ origin are $(E_2 - E_1)/\xi = 5.44$ and $(E_3 - E_1)/\xi = 11.96$.

Similarly, for the low-spin state related to solution, we obtain

$$g_\parallel = 2.224, \quad g_\perp = 1.952$$

$$A = 0.086, \quad B = 0.995, \quad \mu/\xi = -8.6$$

$$(E_2 - E_1)/\xi = 7.98, \quad (E_3 - E_1)/\xi = 9.10$$

In both cases the large value of B indicates that the ground-state Kramers doublet consists essentially of the state wherein the unpaired electron remains in the d_{xy} orbital. The rhombic distortion vanishes in solution, while the axial distortion remains almost unaffected so that the ground state is not modified. It is also apparent that the ground-state doublet is well-separated from the first excited state with a spacing of 5.44ξ in the rhombic case and 7.98ξ in the axial case. Obviously, neither the first nor the second excited-state doublet can be thermally populated and the low-spin magnetic moment is expected to be temperature independent. In conjunction with the fact that the magnetic contribution of the $^6A_{1g}$ state can be also considered as temperature independent except at low temperatures, this has two consequences. First, the temperature dependence of the experimental magnetic

(41) Tweedle, M. F.; Wilson, L. J. *J. Am. Chem. Soc.* **1976**, *98*, 4824.
(42) Wickman, H. H.; Klein, M. P.; Shirley, D. A. *J. Chem. Phys.* **1965**, *42*, 2113.
(43) Bohan, T. L. *J. Magn. Reson.* **1977**, *26*, 109.

moment has to be attributed solely to spin-crossover origins. Then some support is given to the model used in fitting the μ vs T data and based on a Boltzmann distribution over two states, each characterized by a constant moment.

Finally, there is no doubt that, in spite of some weak differences between powdered sample and solution, the magnetic properties of $[(AE)_2Fe]^+$ must be described in terms of high-spin ($S = {}^5/_2$) to low-spin ($S = {}^1/_2$) conversion, in both cases. The studies of the anomalies observed for ground crystals will be the subject of a future examination.

Registry No. $[(AE)_2Fe]BPh_4$, 127182-79-0.

Supplementary Material Available: Tables of atomic coordinates, thermal parameters, bond lengths and angles, and least-squares planes (5 pages); a structure factor table (19 pages). Ordering information is given on any current masthead page.

Contribution from the Department of Chemistry, Columbia University, New York, New York 10027

(Tris(3-*tert*-butylpyrazolyl)hydroborato)manganese(II), -iron(II), -cobalt(II), and -nickel(II) Halide Derivatives: Facile Abstraction of Fluoride from $[BF_4]^-$

Ian B. Gorrell and Gerard Parkin*

Received November 7, 1989

The complexes $\{\eta^3\text{-HB(3-Bu}^t\text{pz)}_3\}$MCl (M = Mn, Fe, Co, Ni) have been prepared by metathesis of MCl_2 with $Tl\{HB(3\text{-Bu}^t\text{pz})_3\}$. Reaction of $\{\eta^3\text{-HB(3-Bu}^t\text{pz)}_3\}$MCl (M = Fe, Co) with $AgBF_4$ results in fluoride abstraction and the formation of $\{\eta^3\text{-HB(3-Bu}^t\text{pz)}_3\}$MF. The molecular structures of the complexes $\{\eta^3\text{-HB(3-Bu}^t\text{pz)}_3\}$FeCl, $\{\eta^3\text{-HB(3-Bu}^t\text{pz)}_3\}$CoCl, and $\{\eta^3\text{-HB(3-Bu}^t\text{pz)}_3\}$CoF have been determined by single-crystal X-ray diffraction studies. Crystal data for $\{\eta^3\text{-HB(3-Bu}^t\text{pz)}_3\}$FeCl: $C_{21}H_{34}N_6BFeCl$; a = 16.075 (5), b = 15.958 (4), c = 9.792 (4) Å; orthorhombic, space group *Pnma* (No. 62); Z = 4. Crystal data for $\{\eta^3\text{-HB(3-Bu}^t\text{pz)}_3\}$CoCl: $C_{21}H_{34}N_6BCoCl$; a = 16.024 (1), b = 15.966 (3), c = 9.769 (4) Å; orthorhombic, space group *Pnma* (No. 62); Z = 4. Crystal data for $\{\eta^3\text{-HB(3-Bu}^t\text{pz)}_3\}$CoF: $C_{21}H_{34}N_6BCoF$; a = 18.402 (5), b = 15.414 (6), c = 9.722 (1) Å; β = 100.24 (3)°; monoclinic, space group *P*1*n*1 (No. 7); Z = 2.

Introduction

The coordination chemistry of poly(pyrazolyl)hydroborato ligands with the transition metals has developed extensively since their introduction by Trofimenko.[1] In particular, the tris(pyrazolyl)hydroborato ligand is often considered as a cyclopentadienyl analogue in that both ligands effectively occupy three coordination sites around a metal center and are both 5-electron donors.[2] Alkyl-substituted derivatives of the cyclopentadienyl ligand, and most notably the pentamethylcyclopentadienyl ligand, have been successfully utilized to allow the formation of monomeric transition-metal complexes that may not be accessible for the unsubstituted cyclopentadienyl derivatives. The cone angles of the alkyl-substituted η^3-tris(pyrazolyl)hydroborato ligands η^3-$HB(pz)_3$, η^3-$HB(3,5\text{-Me}_2pz)_3$, and η^3-$HB(3\text{-Bu}^tpz)_3$ have been estimated as 184, 224, and 244°, respectively, and are significantly larger than the cone angles of 100 and 142° for the η^5-C_5H_5 and η^5-C_5Me_5 ligands.[3,4] It is, therefore, to be expected that the greater steric demands of the η^3-tris(pyrazolyl)hydroborato ligands may allow the isolation of unusual derivatives that are not accessible for the cyclopentadienyl counterparts. For example, Curtis et al. have demonstrated that the η^3-$HB(3,5\text{-Me}_2pz)_3$ ligand is capable of stabilizing a 17-electron radical, $\{\eta^3\text{-HB(3,5-Me}_2pz)_3\}Mo(CO)_3$.[5] Here we report the use of the tris(3-*tert*-butylpyrazolyl)hydroborato ligand in the preparation of half-sandwich halide derivatives of manganese, iron, cobalt, and nickel, $\{\eta^3\text{-HB(3-Bu}^t\text{pz)}_3\}$MCl (M = Mn, Fe, Co, Ni).

Results and Discussion

Several (poly(pyrazolyl)hydroborato)iron complexes have been reported, of which the 6-coordinate, 18-electron derivatives $\{\eta^3\text{-HB(pz)}_3\}_2Fe$[6] and $\{\eta^3\text{-HB(3,5-Me}_2pz)_3\}_2Fe$[7] may be viewed as analogues of ferrocene. The effect of increasing the size of the

Table I. Atom Coordinates (×10⁴) and Temperature Factors (Å² × 10³) for $\{\eta^3\text{-HB(3-Bu}^t\text{pz)}_3\}$FeCl

atom	x	y	z	U^a
Fe	1588 (1)	7500	5931 (1)	41 (1)
Cl	256 (1)	7500	5306 (2)	85 (1)
N(11)	3303 (4)	7500	5120 (6)	47 (3)
N(12)	2540 (4)	7500	4490 (6)	47 (2)
N(21)	2981 (3)	8288 (3)	7265 (4)	45 (2)
N(22)	2147 (3)	8446 (3)	4088 (4)	41 (2)
C(11)	3908 (5)	7500	4194 (10)	57 (3)
C(12)	3553 (6)	7500	2924 (10)	64 (4)
C(13)	2700 (5)	7500	3140 (7)	51 (3)
C(14)	1999 (6)	7500	2113 (7)	63 (4)
C(15)	2356 (6)	7500	655 (8)	104 (5)
C(16)	1468 (4)	6718 (4)	2292 (6)	89 (3)
C(21)	3310 (4)	8882 (4)	8060 (5)	58 (2)
C(22)	2705 (4)	9438 (4)	8394 (6)	59 (2)
C(23)	1980 (3)	9152 (4)	7782 (5)	45 (2)
C(24)	1114 (4)	9534 (4)	7865 (5)	53 (2)
C(25)	512 (3)	8889 (4)	8435 (5)	61 (2)
C(26)	1133 (4)	10289 (4)	8851 (7)	100 (3)
C(27)	843 (4)	9826 (4)	6464 (6)	102 (3)
B	3391 (6)	7500	6668 (9)	46 (3)

[a] Equivalent isotropic U defined as one-third of the trace of the orthogonalized U_{ij} tensor.

Table II. Bond Lengths (Å) for $\{\eta^3\text{-HB(3-Bu}^t\text{pz)}_3\}$FeCl

Fe-Cl	2.227 (2)	Fe-N(12)	2.083 (6)
Fe-N(22)	2.091 (4)	Fe-N(22′)	2.091 (4)
N(11)-N(12)	1.373 (9)	N(11)-C(11)	1.329 (11)
N(11)-B	1.522 (11)	N(12)-C(13)	1.347 (9)
N(21)-N(22)	1.375 (6)	N(21)-C(21)	1.335 (7)
N(21)-B	1.535 (7)	N(22)-C(23)	1.343 (7)
C(11)-C(12)	1.368 (13)	C(12)-C(13)	1.388 (13)
C(13)-C(14)	1.509 (12)	C(14)-C(15)	1.538 (11)
C(14)-C(16)	1.523 (9)	C(14)-C(16′)	1.523 (9)
C(21)-C(22)	1.356 (9)	C(22)-C(23)	1.388 (8)
C(23)-C(24)	1.521 (8)	C(24)-C(25)	1.519 (8)
C(24)-C(26)	1.545 (9)	C(24)-C(27)	1.512 (8)
B-N(21′)	1.535 (7)		

(1) (a) Trofimenko, S. *Acc. Chem. Res.* **1971**, *4*, 17-22. (b) Trofimenko, S. *Chem. Rev.* **1972**, *72*, 497-509. (c) Trofimenko, S. *Prog. Inorg. Chem.* **1986**, *34*, 115-210. (d) Shaver, A. *Comprehensive Coordination Chemistry*; Wilkinson, G., Gillard, R. D.; McCleverty, J. A., Eds.; Pergamon Press: Oxford, England, 1987; Vol. 2, pp 245-259. (e) Shaver, A. *J. Organomet. Chem. Libr.* **1977**, *3*, 157-188.

(2) Electron counting is according to a neutral ligand formalism.

(3) Trofimenko, S.; Calabrese, J. C.; Thompson, J. S. *Inorg. Chem.* **1987**, *26*, 1507-1514.

(4) (a) Frauendorfer, E.; Brunner, H. *J. Organomet. Chem.* **1982**, *240*, 371-379. (b) Davies, C. E.; Gardiner, I. M.; Green, J. C.; Green, M. L. H.; Hazel, N. J.; Grebenik, P. D.; Mtetwa, V. S.; Prout, K. *J. Chem. Soc., Dalton Trans.* **1985**, 669-683.

(5) Shiu, K.-B.; Curtis, M. D.; Huffman, J. C. *Organometallics* **1983**, *2*, 936-938.

(6) Trofimenko, S. *J. Am. Chem. Soc.* **1967**, *89*, 3148-3158.

0020-1669/90/1329-2452$02.50/0